7.1 EFFECT OF STRAIN FIELD ON THRESHOLD DISPLACEMENT ENERGY OF TUNGSTEN STUDIED BY MOLECULAR DYNAMICS SIMULATION —

D. Wang, N. Gao, (Institute of Modern Physics, Chinese Academy of Sciences) W. Setyawan, R. J. Kurtz (Pacific Northwest National Laboratory), X. Gao, W. H. He (Institute of Modern Physics, Chinese Academy of Sciences)

OBJECTIVE

The objective of this research is to support the interpretation of irradiation damage properties of bulk tungsten-based materials using computational methods. In particular, to provide quantitative information on the directional and strain dependencies of the point defect and threshold displacement energies in bulk tungsten.

SUMMARY

The influence of hydrostatic strain on point defect formation energy and threshold displacement energy (E_d) in body-centered cubic (BCC) tungsten was studied with molecular dynamics simulations. Two different tungsten potentials (Fikar and Juslin) were used. The minimum E_d direction calculated with the Fikar-potential was <100>, but with the Juslin-potential it was <111>. The most stable self-interstitial (SIA) configuration was a <111>-crowdion for both potentials. The stable SIA configuration did not change with applied strain. Varying the strain from compression to tension increased the vacancy formation energy but decreased the SIA formation energy. The SIA formation energy changed more significantly than for a vacancy such that E_d decreased with applied strain from compression to tension.

CONDENSATION OF A PAPER SUBMITTED FOR PUBLICATION[1]

Methods

The potentials fitted by Juslin and Wirth [1] and Fikar and Schaublin [2] were used in the present work. In the following text, the notation Juslin-potential and Fikar-potential represent these two potentials, respectively. Both potentials are modifications of the Ackland-Thetford (AT) potential [3]. The Juslin-potential gives properties for SIA defects closer to densify functional theory (DFT) results [4,5] than the Fikar-potential. The potentials differ mainly in their treatment of the connection between the Ziegler-Biersack-Littmark (ZBL) potential [6] and the AT potential. Molecular dynamics (MD) simulations were performed using the Large-scale Atomic/Molecular Massively Parallel Simulator (LAMMPS) code [7]. Periodic boundary conditions were applied in all directions. The effect of an applied hydrostatic strain on various point defect formation energies and E_d was studied. Six configurations of a point defect were explored; 1) vacancy, 2) <111>-crowdion (crowd111), 3) <100>-dumbbell (db100), 4) <110>-dumbbell (db110), 5) octahedral (oct) interstitial, and 6) tetrahedral (tetra) interstitial.

Threshold displacement energies were determined by constructing simulation cells designed to keep the displacement cascade near the cell center. A 30×30×30 BCC lattice containing 54000 tungsten atoms was used for <100> and <110> directions, and a 40×40×40 BCC lattice containing 128000 tungsten atoms for the <111> direction. The simulation cell was divided into two regions by fixing two atomic layers adjacent to the cell surface, denoted as Region-I, and the remaining volume was designated as Region-II, as shown in Figure 1. During the simulation, NVT and NVE ensembles were used for these two regions, respectively. Periodic boundary conditions were applied in all directions. For each direction, six different primary knock-on atoms (PKAs) were selected to calculate the average E_d value. Small hydrostatic strains ranging from -2% to 2% were applied to the simulation cell along the principal directions. The cell was first relaxed under the preset strain by setting T=10 K using an NVT ensemble. After this relaxation, a displacement cascade was created in Region-II with an NVE ensemble while keeping T=10K in Region-I with NVT. In each case, the total simulation time was about 6 ps. If a Frenkel pair existed after 6 ps, then it was regarded as a stable defect. The Wigner-Seitz cell and common-

[1] Paper submitted for publication in the Journal of Nuclear Materials.

neighbor analysis methods were used to analyze the various defect configurations and found to give the same results for E_d.

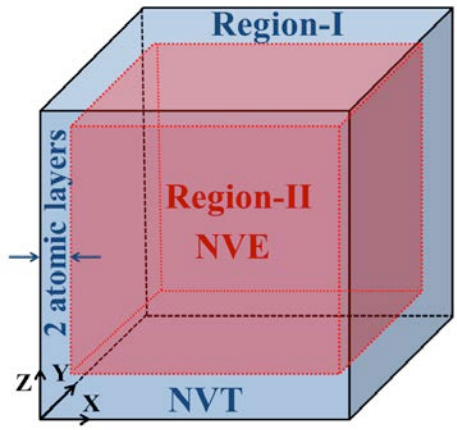

Figure 1. Schematic of the simulation cell used in the present work. Region-I is the border region, which contains 2 atomic layers from each of the box boundaries. Region-II is the active region. NVT and NVE ensembles are used in Region-I and II, respectively.

Results

Defect formation energy

The formation energies of the six point defects without strain were computed as a reference case. The results are listed in Table 1. Both potentials show that the most stable SIA configuration is a <111>-crowdion, which is also found by DFT [4,5] and the AT [3] potential. For a vacancy, both potentials give the same formation energy, which is approximately equal to DFT values [4,5,8]. The interstitial formation energies obtained from the Fikar-potential are close to AT potential results, while the values calculated with the Juslin-potential are close to DFT values, even though the Juslin-potential is derived from the AT potential.

When strain is applied, both potentials show that the <111>-crowdion is still the most stable SIA, as shown in Figure 2. In Figure 2, negative values represent a compressive strain. Under a compressive strain the octahedral and tetrahedral interstitials are unstable. The octahedral interstitial transforms to a <100>-dumbbell, and the tetrahedral interstitial transforms to an imperfect octahedral configuration when the magnitude of the strain is greater than about 1.0% in both cases. Vacancy and interstitial defects respond differently to applied strain as shown in Figure 2. The vacancy formation energy increases slowly as the strain changes from compressive to tensile. Under a compressive strain the local tensile stress around the vacant site decreases making vacancy formation easier. A tensile strain does the opposite, but only to a smaller degree. At 2% tensile strain, the vacancy formation energy increased only about 3%. For SIAs, the formation energy decreases rapidly with strain state from compression to tension. An interstitial induces local compressive stresses, which increases the potential energy of the system. Thus, a tensile strain reduces these stresses, decreasing the interstitial formation energy.

Table 1. The formation energies, E_f, of point defects in tungsten calculated with the Fikar-potential and the Juslin-potential. Results obtained from DFT and the AT potential are also listed.

E_f, eV	DFT	AT-Potential	Fikar-Potential	Juslin-Potential
vac	3.68 [8] 3.56 [4,5]	-	3.63	3.63
oct	11.68 [4,5]	-	9.98	10.41
tetra	11.05 [4,5]	-	9.97	10.46
crowd111	9.55 [4,5]	8.88 [3]	8.87	9.54
db100	11.49 [4,5]	9.82 [3]	9.79	10.28
db110	9.84 [4,5]	9.64 [3]	9.62	10.18

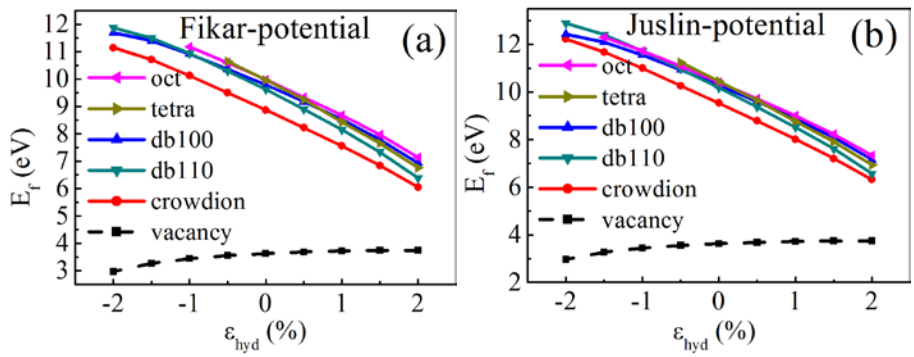

Figure 2. Strain dependence of the formation energies of point defects E_f in W calculated with (a) the Fikar-potential and (b) the Juslin-potential. A negative value represents a compressive strain.

Threshold displacement energy

Threshold displacement energies were determined along the <100>, <110> and <111> directions. The results at zero strain are listed in Table 2. Other simulation results and experimental measurements are also given. Since the <111>-crowdion is the most stable SIA configuration, the majority of defects produced in a displacement cascade should be <111>-crowdions and vacancies, and the minimum E_d should be along a <111> direction. However, results obtained with the Fikar-potential show that the minimum E_d is about 64 eV along a <100> direction. In contrast, the minimum E_d for the Juslin-potential is along a <111> direction, at about 43 eV, even though the <100> direction E_d is very close to the Fikar-potential result. Simulations done by Stuart [9] gave a minimum E_d of 65.6 eV along a <100> direction, in agreement with our Fikar-potential results. The electron irradiation experimental result reported by Maury [10] also found the minimum E_d direction to be <100>. Interestingly, the experimental data show only a small difference between <100> and <111> E_d values, unlike the computed results.

Table 2. The displacement threshold energy, E_d, values for the <100>, <111> and <110> directions in tungsten calculated with the Fikar-potential and the Juslin-potential. Electron irradiation results by Maury [10] and computer simulation results by Stuart [9] are presented for comparison.

E_d, eV	<100>	<111>	<110>
Fikar-potential	64 ± 1	70 ± 1	209 ± 7
Juslin-potential	63 ± 1	43 ± 1	164 ± 22
Maury [10]	42 ± 2	44 ± 1	75 ± 5
Stuart [9]	65.6 ± 0.1	~250	~100

When strain is applied, the threshold displacement energies are considerably affected, as presented in Figure 3. The results show that E_d decreases with strain from compression to tension for both potentials. The trend is the same for all three directions and the minimum E_d direction did not change with strain. The results suggest that when tungsten is loaded in hydrostatic compression, more energy will be needed to create a stable Frenkel pair, that is, a pre-compressive stress might increase radiation damage resistance in tungsten, assuming the pre-stress does not rapidly relax at service temperatures.

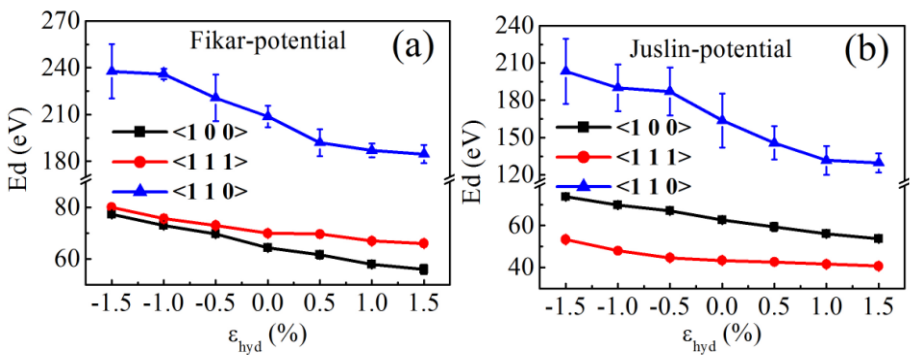

Figure 3. Strain dependence of the E_d values for the <100>, <111> and <110> directions in tungsten simulated with (a) the Fikar-potential and (b) the Juslin-potential.

Conclusions

Molecular dynamic simulations were used to compute the effect of strain on point defect formation and threshold displacement energies in tungsten. The most stable SIA point defect is a <111>-crowdion with or without an applied hydrostatic strain. The formation energies of SIAs decreased rapidly, while the vacancy formation energy increased slowly with the applied strain increasing from 2% compression to 2% tension. The E_d values for <100>, <110>, and <111> directions decreased over the same strain range. The direction of the minimum E_d depended on the choice of interatomic potential. The Fikar-potential gave the minimum E_d along a <100> direction, while the Juslin-potential indicated the minimum E_d is along a <111> direction. When strain is applied, the minimum E_d direction did not change.

Acknowledgements

This work was supported by the National Natural Science Foundation of China (NSFC) (Grant Nos. 11375242, 91026002, 91426301). WS and RJK acknowledge the support of the Office of Fusion Energy Sciences, U.S. Department of Energy under Contract DE-AC05-76RL01830.

References

[1] N. Juslin, B.D. Wirth, J. Nucl. Mater., 432 (2013) 61-66.
[2] J. Fikar, R. Schaublin, J. Nucl. Mater., 386-388 (2009) 97-101.
[3] G.J. Ackland, R. Thetford, Philos. Mag. A, 56 (1) (1987) 15-30.
[4] D. Nguyen-Mahn, A.P. Horsfield, S.L. Dudarev, Phys. Rev. B, 73 (2006) 020101(R).
[5] P.M. Derlet, D. Nguyen-Manh, S.L. Dudarev, Phys. Rev. B, 76 (5) (2007) 054107.
[6] J.F. Ziegler, J.P. Biersack, U. Littmark, The Stopping and Range of Ions in Matter, Pergamon, New York, 1985.
[7] S. Plimpton, J. Comp. Phys., 117 (1995) 1-19, http://lammps.sandia.gov.
[8] D. Kato, H. Iwakiri, K. Morishita, J. Nucl. Mater., 417 (2011) 1115-1118.
[9] R.N. Stuart, M.W. Guinan, R.J. Borg, Radiat. Eff., 30 (1976) 129-133.
[10] F. Maury, M. Biget, P. Vajda, A. Lucasson, P. Lucasson, Radiat. Eff., 38 (1978) 53-65.